

Research Journal of Pharmaceutical, Biological and Chemical Sciences

Corrosion Inhibition of Petroleum Pipelines During Acidization Process by N-Dodecan-Diyl-1, 2-Ethane Bis- Dimethyl Ammonium Bromide

AS Fouda¹, MA Migahed^{2*}, AA Atia³, and IM Mosa⁴.

¹Department of Chemistry, Faculty of Science, Mansoura University, Egypt

²Egyptian petroleum research institute, Nasr city, Cairo, Egypt

³Department of Chemistry, Faculty of Science, Zagazig University, Egypt

⁴Agricultural researches center, Egypt.

ABSTRACT

The inhibition efficiency of the cationic gemini surfactant; namely, N-dodecan-diyl-1,2-ethane bis dimethyl ammonium bromide on the corrosion of carbon steel in 1.0 M HCl solution has been evaluated at 30°C by weight loss, Potentiodynamic polarization, EIS and electrochemical frequency modulation (EFM) techniques. The nature of protective film was examined using SEM and EDX techniques. The results of weight loss showed that the inhibition efficiency increases with increasing the inhibitor concentration until the critical micelle concentration (CMC) reached, while it decreases with raising temperature. Changes in impedance parameters; charge transfer resistance, R_{ct} , and double-layer capacitance, C_{dl} , indicated that the adsorption of the compound on the metal surface, leading to the formation of a protective film.

The Potentiodynamic polarization measurements revealed that the adsorption of inhibitor affects both the anodic and cathodic reactions. Finally, some quantum chemical calculations were used to support the experimental data.

Keywords: Corrosion; Carbon steel; Surfactant; Potentiodynamic polarization; EIS; EFM; SEM; EDX and Quantum chemical calculations.

**Corresponding author*

INTRODUCTION

Carbon steel is being used extensively under different condition in industries because it's low cost and prime mechanical properties. However some corrosion problems take place due to the use of acid for pickling of metals, acidization process of old oil wells, and the chemical cleaning of heat exchangers [1]. To decrease the metallic corrosion in acidic media, several techniques have been applied. However, one of the most important methods is the use of organic compounds and more specifically cationic surfactants which are gaining high attention as corrosion inhibitors. This can be attribute to the fact that, surfactants are very salutary reagents and their presence at very low quantity in any medium providing eligible properties to processes in all industries such as painting and coating industry, petrochemical and food [2]. As a new generation of surfactants, Gemini surfactants have attracted great interest in recent years. This kind of surfactant contains two hydrophilic groups and two hydrophobic groups in the molecule separated with a robust or pliable spacer rather than one hydrophilic group and one hydrophobic group for common surfactants [3]. Many Gemini surfactants have been synthesized and abundant numbers of investigations have been reported on their unusual physicochemical properties including their high surface activity, unusual changes of viscosity, unusual micelle structure and perverse aggregation behaviors [4-10]. In general cationic surfactants and particularly Gemini surfactant have effective inhibitory effect, they accumulate in special order at the interfaces and modify the interfaces and thus control, reduce, or prevent reactions between a substrate and its surroundings when added to the medium in small quantities [11]. In this study, weight loss, Potentiodynamic polarization measurements, scanning electron microscopy (SEM) and Energy Dispersion analysis of X-Ray(EDX) were performed to investigate the structural inhibitive effect of this inhibitor on the corrosion process of carbon steel in 1.0 M HCl acid solution. The adsorption mechanism of the Gemini cationic surfactant onto the carbon steel surface was explained.

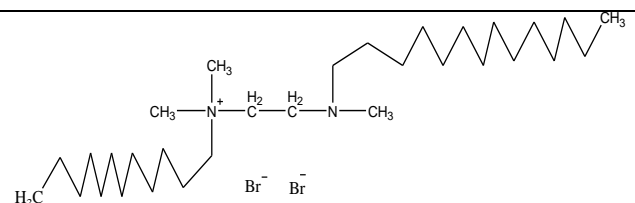
The present paper is aimed to study the corrosion inhibition efficiency of the cationic Gemini surfactant namely, N-dodecan-diyl-1,2-ethane bis dimethyl ammonium bromide,

EXPERIMENTAL

Materials and Solutions:

The specification of the used inhibitor is listed in Table 1. The concentration range of the prepared cationic Gemini surfactant was from 25-150 ppm used for corrosion measurements. All solutions were prepared using distilled water. The aggressive solution, 1.0 M HCl, was prepared by dilution of analytical grade 37 %HCl with distilled water. The concentration range of the prepared cationic Gemini surfactant was from 25-150 ppm used for corrosion measurements. All solutions were prepared using distilled water.

Table 1: Molecular structure, IUPAC name, molecular weight and molecular formula of investigated surfactant.

MolecularStructure	IUPAC Name	Molecular weight	Molecular formula
	N-dodecan-diyl-1,2-ethane bis dimethyl ammonium bromide	614.66	C ₃₀ H ₆₆ Br ₂ N ₂

The chemical composition of carbon steel alloy used in this study is listed in [Table 2](#).

Table 2: Composition of carbon steel alloy

Element	C	Mn	P	Si	Fe
Percentage (wt / wt %)	0.200	0.350	0.024	0.003	Rest

Methods:**Weight loss measurements:**

Rectangular specimens of carbon steel of size (21 mm × 22 mm × 1.5 mm) were abraded with emery paper grit sizes 320, 600, 1000 and 1800, degreased with acetone. Then rinsed several times with bi-distilled water, and finally dried between two filter papers. The weight loss measurements were carried out in a 100 ml capacity glass beaker placed in water thermostat bath. The specimens were then immediately immersed in the test solution containing 1.0 M HCl with and without different concentrations of the investigated Gemini surfactant. After different immersion times (each of 30 min till 150 min), the carbon steel sheets were taken out, rinsed thoroughly with distilled water, dried, and weighed accurately, Triplicate specimens were exposed for each condition and the average weight losses were reported. The weight loss values are used to calculate the corrosion rate using the following equation (1) [12].

$$CR = \frac{K \times W(\text{mg})}{T(\text{h}) \times A(\text{cm}^2) \times D(\text{g/cm}^3)} \dots\dots\dots (1)$$

Where CR is the corrosion rate, K is constant, W is the mass loss (mg), T is the corrosion period (hr), A is the specimen area Cm^2 and D is the density (g/Cm^3). The inhibition efficiency (η %) and degree of metal surface coverage (θ) have been calculated according to the following equation (2) [13].

$$\eta \% = \theta \times 100 = [(CR^* - CR) / CR] \times 100 \dots\dots\dots (2)$$

Where η is the percentage inhibition efficiency, CR^* and CR are the corrosion rate in absence and presence of a definite concentration of the investigated inhibitor, respectively.

Electrochemical measurements:

Electrochemical measurements were conducted in a conventional three electrodes thermostatic cell assembly using a Gamry potentiostat/galvanostate/ZRA (model PCI 300/4). A platinum foil and saturated calomel electrode (SCE) were used as counter and reference electrodes, respectively. The carbon steel electrode was in the form of a square cut from C-steel electrode with exposed surface area 1.0 cm^2 and was welded from one side to a copper wire used for electrical connection. The working electrode was polished successively with different grades of emery paper, washed with bi-distilled water and then degreased with acetone. All experiments were carried out at temperature $(30 \pm 1^\circ\text{C})$.

Potentiodynamic polarization measurements:

The Potentiodynamic curves were recorded from -500 to 500 mV at a scan rate 1 mVs^{-1} after the steady state is reached (30 min) and the open circuit potential (OCP) was recorded. The percentage inhibition efficiency (η %) and the degree of surface coverage (θ) were calculated from Eq. (3).

$$\eta \% = \theta \times 100 = \{1 - (i_{\text{corr}}^0 / i_{\text{corr}})\} \times 100 \dots\dots\dots (3)$$

Where i_{corr}^0 and i_{corr} are the corrosion current densities of uninhibited and inhibited solution, respectively.

Electrochemical Impedance Spectroscopy Technique:

Electrochemical impedance spectroscopy (EIS) measurements were carried out using the same instrument as before with a Gamry frame work system based on ESA400. Gamry applications include software EIS300 for EIS measurement; computer was used for collecting data. Echem Analysis 5.5 software was used for plotting, graphing and fitting data. EIS measurements were carried out in a frequency range of 100 kHz to 10 mHz with amplitude of 5.0 mV peak-to-peak using ac signals at respective corrosion potential. The inhibition efficiency (η %) of the inhibitor has been found out from the charge transfer resistance values using the following equation (4) [14].

$$\eta_{EIS} \% = \theta \times 100 = (R_{ct} - R_{ct}^0) / R_{ct} \times 100 \dots\dots\dots (4)$$

Where R_{ct}^0 and R_{ct} are the charge transfer resistance in the absence and presence of the inhibitor respectively. The interfacial double layer capacitance (C_{dl}) values were obtained by the impedance value [15] by the following equation (5):

$$C_{dl} = 1 / 2\pi R_{ct} f \dots\dots\dots (5)$$

Where R_{ct} is the charge transfer resistance and f is the frequency (Hz).

Electrochemical Frequency Modulation Technique (EFM):

EFM can be used as a rapid and nondestructive technique for corrosion rate measurements without prior knowledge of Tafel constants. EFM carried out using two frequencies 2.0 and 5.0 Hz. The base frequency was 0.1 Hz. In this study, we use a perturbation signal with amplitude of 10.0 mV for both perturbation frequencies of 2.0 and 5.0 Hz. Equilibrium time leading to steady state of the specimens was 30 min. η_{EFM} was calculated using the following equation (6):

$$\eta \% = [(i_{corr}^0 - i_{corr}) / i_{corr}^0] * 100 \dots\dots\dots(6)$$

Where i_{corr}^0 and i_{corr} are corrosion current densities in the absence and presence of inhibitor, respectively

Scanning Electron Microscopy (SEM-EDX):

The surface morphology measurements of the carbon steel surface were carried out using scanning electron microscopy (SEM) into the spectrometer Philips (pw-1390) with Cu-tube (Cu kal, $1= 1.54051A^\circ$), a scanning electron microscope (SEM, JOEL, JSM-T20, Japan) and Emission dispersive X-ray analysis (EDX) Model HITACHI S-3000H.

Theoretical study:

All the quantum chemical calculations were performed using Materials Studio [16] version 4.4.0. The following quantum chemical indices were considered: HOMO energy (highest occupied molecular orbital), LUMO energy (lowest unoccupied molecular orbital), dipole moment (μ), energy gap, ΔE ($\Delta E = E_{LUMO} - E_{HOMO}$) and Mulliken charge of the investigated inhibitor.

RESULTS AND DISCUSSION

Weight loss measurements:

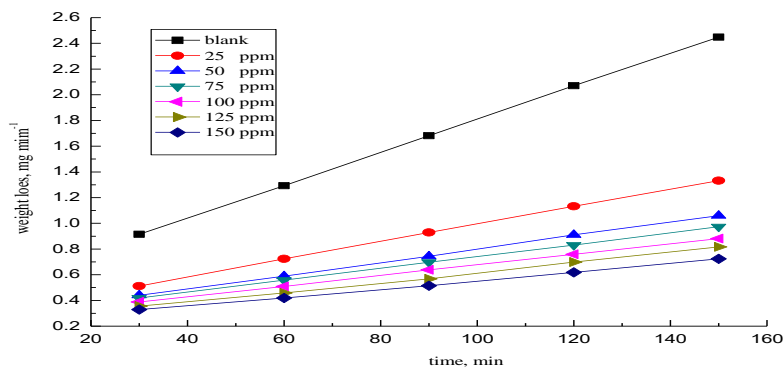


Fig. 1: weight loss curve for carbon steel dissolution in 1.0 M HCl in absence and presence of different concentration of the surfactant inhibitor at 30°C.

The weight loss-time curves of C-steel immersed in 1.0 M HCl solution only (blank) and that injected with various doses of N-dodecan-diyl-1,2-ethane bis dimethyl ammonium bromide are shown in Fig. 1. The data obtained from weight loss measurements are summarized in Table 3.

Table 3: Data obtained from weight loss measurements for C-steel in 1.0 M HCl solution in absence and presence of different concentration of the surfactant inhibitor at 150 min. immersion and 30°C

Conc., ppm	CR (mg Cm ⁻² min ⁻¹) x10 ⁻³	θ	η %
0.0	12.8	----	----
25	6.83	0.466	46.6
50	5.19	0.594	59.4
75	4.61	0.639	63.9
100	4.12	0.677	67.7
125	3.87	0.697	69.7
150	3.3	0.742	74.2

A decrease in the weight loss of C-steel in the presence of various concentration of the undertaken surfactant is observed as a general trend even at a low concentration compared with the surfactant free solution. The results show that the tested surfactant acts as a good corrosion inhibitor for C-steel in 1.0 M HCl. Also, the obtained data (Table 3) shows an increase in the corrosion inhibition efficiency with increasing in the surfactant concentration at a constant temperature. Generally, it is acceptable to attribute the primary action in the inhibition process by surfactant is the adsorption of the surfactant molecules via their functional group onto the metal surface.

Electrochemical measurements:

Potentiodynamic polarization technique:

The Potentiodynamic curves for C- steel in 1.0 M HCl in the absence and presence of different concentrations of the inhibitor at 30° C were shown in Fig. 2. It is clear from the obtained curves that; the corrosion current obtained for the test C-steel in the presence of surfactant molecules is lower than inhibitor free solution, i.e. blank. This lower in corrosion current values for inhibitor solution confirm that the rate of electrochemical reaction is reduced due to the formation of a barrier layer over the carbon steel surface by the inhibitor molecules [17] the data report in Table 4.also reveals that E_{corr} values of inhibited and uninhibited system do not vary significantly indicating that both anodic and cathodic reaction are affected by the addition of the studied surfactant. This behavior imply that the studied cationic Gemini surfactant acts as mixed type inhibitor i.e. promoting retardation of both anodic dissolution of C-steel and cathodic hydrogen discharge reaction [18,19].

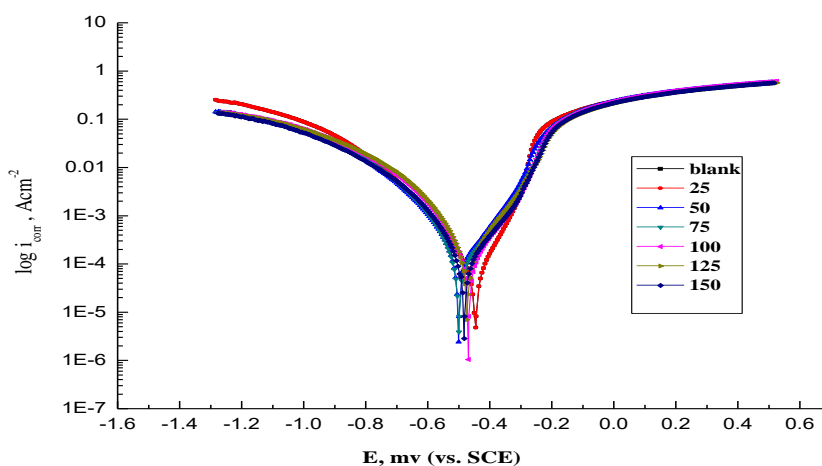


Fig. 2: Potentiodynamic polarization curves for the dissolution of C- steel in 1.0 M HCl in the absence and presence of different concentrations of the surfactant inhibitor at 30°C.

Table 4: Potentiodynamic data of C-steel in 1.0 M HCl and in the presence of different concentration of the inhibitor at 30°C.

Compound	Conc., ppm	E_{corr} -vs.SCE, mV	i_{corr} , mA	$-\beta_c$, mV dec ⁻¹	$-\beta_a$, mV dec ⁻¹	θ	$\eta\%$
N-dodecan-diy-1,2-ethane bis dimethyl ammonium bromide	0.0	435	1.73	147	92	-----	-----
	25	474	0.719	206.8	133.7	0.584	58.4
	50	463	0.609	201.1	126.1	0.648	64.8
	75	465	0.531	168	120.1	0.693	69.3
	100	477	0.486	193.6	122.6	0.719	71.9
	125	477	0.421	171.3	117.3	0.756	75.6
	150	479	0.383	193.4	119.8	0.778	77.8

Both cathodic Tafel slopes (β_c) and anodic Tafel slopes (β_a) do not change remarkably, which indicates that the mechanism of the corrosion reaction does not change and the corrosion reaction is inhibited by simple adsorption mode [20]. The irregular trends of β_a and β_c values indicate the involvement of more than type of species adsorbed on the metal surface. Generally; the increase of the inhibitor concentration shifts corrosion potential into a less negative direction, what can be explained by a small domination of anodic reaction inhibition.

Electrochemical impedance spectroscopy:

The EIS provides important mechanistic and kinetic information for an electrochemical system under investigation. Nyquist impedance plots obtained for the C-steel electrode at respective corrosion potential after 30 min immersion in 1.0 M HCl at 30°C in absence and presence of various concentrations of the inhibitor as it shown in Fig.3. The curves show a similar type of Nyquist plots for carbon steel in the presence of various concentrations of the inhibitor. The existence of single semi-circle showed the single charge transfer process during dissolution which is unaffected by the presence of inhibitor molecules.

The deviations of The Nyquist plots of the inhibitor from perfect semicircles as expected from the theory of EIS. The impedance loops measured are depressed semi-circles with their centers below the real axis, where the kind of phenomenon is known as the dispersing effect as a result of frequency dispersion [21] and mass transport resistant [22] as well as electrode surface heterogeneity resulting from surface roughness, impurities, dislocations, grain boundaries, adsorption of inhibitor, and formation of porous layers [23-27], so one constant phase element (CPE) is substituted for the capacitive element, to explain the depression of the capacitance semi-circle, to give a more accurate fit. Impedance data are analyzed using the circuit in Fig.3.5; in which R_s represents the solution resistance, R_{ct} represents the charge- transfer resistance and C_{dl} represents the double layer capacitance. According to Hsu and Mansfeld [28] the correlation of capacity to its real values is calculated from Eq. (7)

$$C_{dl} = Y_o (\omega_{max})^{n-1} \dots\dots\dots(7)$$

Where Y_o is the CPE coefficient and ω_{max} is the frequency at which imaginary part of the impedance ($-Z_i$) has a maximum and n is the CPE exponent (phase shift).The data obtained from fitted spectra are listed in Table 5. The $\eta\%$ was calculated from the above mentioned Eq. (4). It is clear that, the (R_{ct}) values increases and the (C_{dl}) values decreases by increasing the inhibitor concentrations, which causes an increase of θ and η . This is due to the gradual replacement of water molecules by the adsorption of the inhibitor molecules on the metal surface, decreasing the extent of dissolution reaction. The higher (R_{ct}) values, are generally associated with slower corroding system[22] The decrease in the (C_{dl}) can result from the decrease of the local dielectric constant and/or from the increase of thickness of the electrical double layer suggested that the inhibitor molecules function by adsorption at the metal/solution interface [29].

The inhibition efficiencies, calculated from EIS show the same trend as those obtained from polarization and weight loss measurements, the difference of inhibition efficiency from the three methods

may be attributed to the difference surface status of the electrode in the three measurements. EIS were performed at the rest potential, while in polarization measurements the electrode potential was polarized to high over potential, non-uniform current distributions, results from cell geometry, solution conductivity, counter and reference electrode placement, etc., will lead to the difference between the electrode area actually undergoing polarization and the total area [30].

The increase of absolute impedance with increasing the injection dose of the cationic surfactant as shown Fig.4, which represent the Bode plots approved gives a direct relation of the adsorption of inhibitor molecules on C-steel surface [31-33]. Furthermore the reduction of phase angle (θ_{max}) at intermediate frequency with increasing inhibitor concentration, which indicated the decrease of capacitive response with the increase of the used surfactant concentration [34]

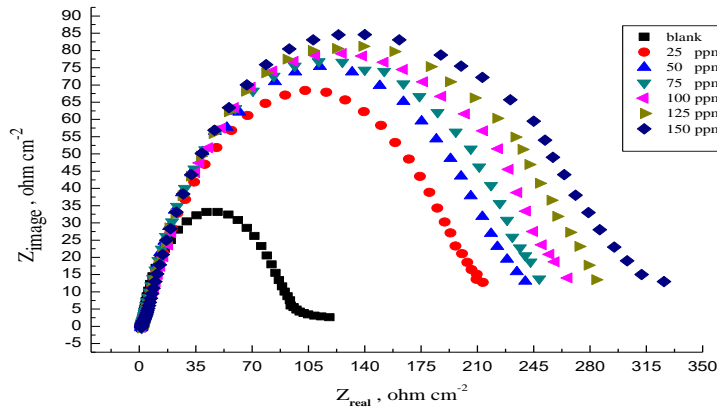


Fig.3: The Nyquist plots for the corrosion of C-steel in 1.0 M HCl in the absence and presence of different concentrations of the surfactant inhibitor at 30°C.

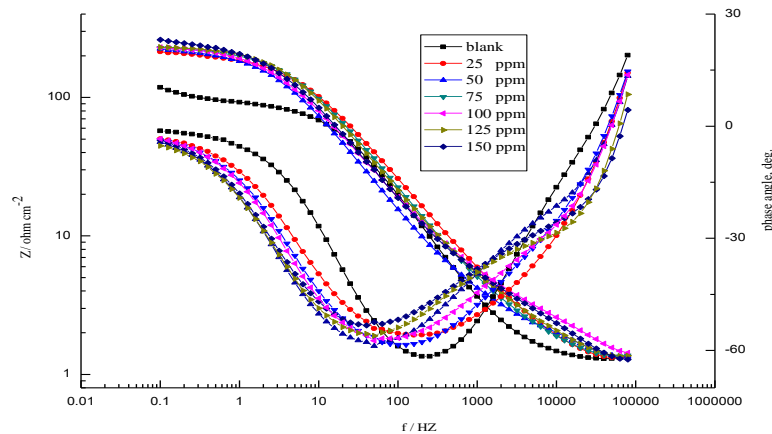


Fig. 4: Bode plots for the corrosion of C-steel in 1.0 M HCl in the absence and presence of different concentrations of the surfactant inhibitor at 30°C.

Table 5: EIS parameters for the corrosion of C-steel in 1.0 M HCl in the absence and presence of different concentrations of inhibitor (gemini) at 30 °C.

Conc. ppm	Cdl, $\mu\text{F cm}^{-2}$	Rct, $\Omega \text{ cm}^2$	θ	% IE
Blank	1.06	95.53	---	---
25	3	212.4	0.550	55.0
50	2.95	237.9	0.598	59.8
75	2.9	249.3	0.616	61.6
100	1.8	265.8	0.640	64.0

125	1.5	283.4	0.663	66.3
150	1.3	318.9	0.700	70.0

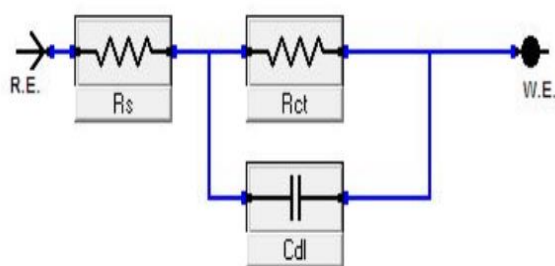


Fig. 5: Electrical equivalent circuit model used to fit the impedance spectra data.

Electrochemical frequency modulation (EFM) measurements:

EFM is a nondestructive corrosion measurement technique like EIS; it is a small signal ac technique. Unlike EIS, however, two sine waves (at different frequencies) are applied to the cell simultaneously. The great strength of the EFM is the causality factors which serve as an internal check on the validity of the EFM measurement [35]. With the causality factors the experimental EFM data can be verified. The results of EFM experiments are a spectrum of current response as a function of frequency. The spectrum is called the inter modulation spectrum. The spectra contain current responses assigned for harmonical and inter modulation current peaks. The larger peaks were used to calculate the corrosion current density (i_{corr}), the Tafel slopes (β_a and β_c) and the causality factors (CF-2 and CF-3). Inter modulation spectra obtained from EFM measurements as presented in Fig.6 for 1.0 M HCl in absence and presence of 150 ppm of the inhibitor Table 3.4.indicated that the corrosion current densities decrease by increasing the concentration of the investigated inhibitor and the inhibition efficiencies % η calculated from eq. (6) increase by increasing the investigated surfactant concentration.

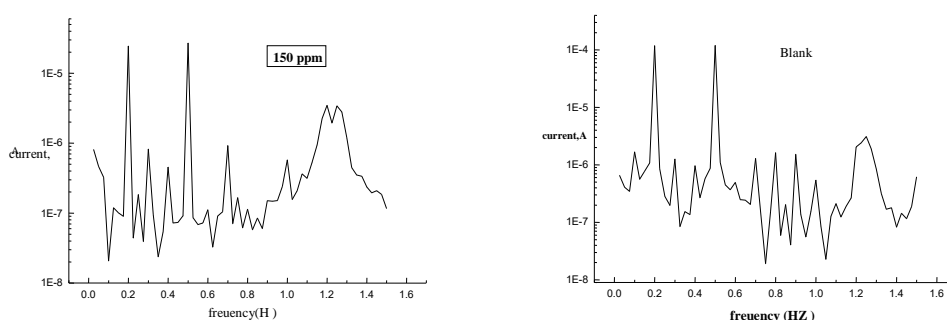


Fig.6: Intermodulation spectra for C- steel in in 1.0 M HCl in the absence and presence of 150 ppm of the surfactant inhibitor.

Table 6: Electrochemical kinetic parameters obtained by EFM technique for C-steel in the absence and presence of various concentrations of the surfactant inhibitor in 1.0 M HCl at 30°C

Compound	Conc., ppm	i_{corr} , $\mu A cm^{-2}$	$-\beta_c$, $mV dec^{-1}$	$-\beta_a$, $mV dec^{-1}$	CF-2	CF-3	% η
N-dodecan-diyl-1,2-ethane bis dimethyl ammonium bromide	0.0	258.2	32.6	26.2	2.5	3.2	-----
	25	113.7	231.7	98.5	2.3	3.1	55.96
	50	115.3	209.6	103.8	2.1	3.2	55.34
	75	100.4	187.9	123.7	2.2	3.3	61.11
	100	84.9	278.9	134.2	2.3	3.1	67.11
	125	68.3	302.9	142.4	2.1	3.2	73.54
	150	59.8	287.6	129.8	2.1	3.1	76.84

The causality factors in Table 6 are very close to theoretical values which according to the EFM theory [36] should guarantee the validity of Tafel slopes and corrosion current densities

Adsorption isotherm:

Adsorption of surfactants on solid surfaces can modify their hydrophobicity, surface charge and other key properties that govern interfacial processes such as corrosion inhibition [37]. In general, adsorption is governed by a number of forces such as covalent bonding, electrostatic attraction, hydrogen bonding or non-polar interaction between the adsorbed species, lateral association interaction, solvation and de-solvation [38]. The total adsorption is usually the cumulative result of some or all of the above forces [39]. Standard free energy of adsorption (ΔG°_{ads}) can be written as [38]:

$$\Delta G^{\circ}_{ads} = \Delta G^{\circ}_{elec} + \Delta G^{\circ}_{chem} + \Delta G^{\circ}_{c-c} + \Delta G^{\circ}_{c-s} + \Delta G^{\circ}_H + \Delta G^{\circ}_{H_2O} + \dots \quad (8)$$

Where ΔG°_{elec} is the electrostatic interaction term, ΔG°_{chem} the chemical term due to covalent bonding, ΔG°_{c-c} the free energy gained upon association of methyl groups in the hydrocarbon chain, ΔG°_{c-s} the free energy due to the interaction between the hydrocarbon chains and hydrophobic sites on the solid, ΔG°_H the hydrogen bonding term and $\Delta G^{\circ}_{H_2O}$ is the term owing to dissolution or solvation of the adsorption species or any species displaced from the interface due to adsorption.

Several adsorption isotherms were assessed and the Langmuir adsorption isotherm was found to be the best description of the adsorption behaviour of the investigated Gemini surfactant which obeys the following equations:

$$C_{inh} / \theta = 1/k + C_{inh} \dots \dots \dots (9)$$

Where, C_{inh} is the inhibitor concentration, θ is the fraction of the surface coverage, k is the modified adsorption equilibrium constant which can be related to the free energy of adsorption (ΔG°_{ads}) as follows:

$$K = 1/C_{solvent} \exp \Delta G^{\circ}_{ads} / RT \dots \dots \dots (10)$$

$C_{solvent}$ is the molar concentration of solvent which in the case of the water is 55.5 mol.L^{-1} .

$$K_{ads} = 1/55.5 \exp [-\Delta G^{\circ}_{ads} / RT] \dots \dots \dots (11)$$

Fig.: Shows that the dependence of the fraction of the surface coverage (C_{inh}/θ) as a function of the concentration (C_{inh}) of the inhibitor.

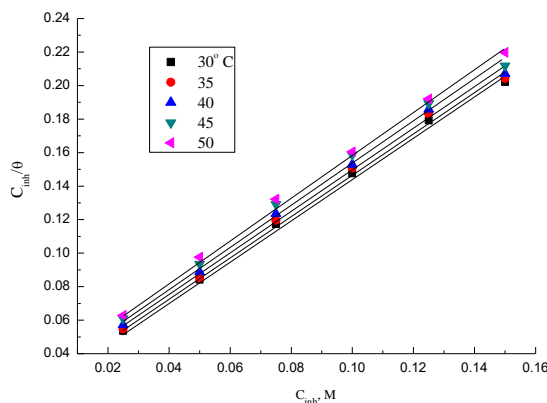


Fig. 7: Langmuir adsorption plots for C-steel in 1.0 M HCl containing various concentrations of the surfactant inhibitor at different temperatures.

Table 7: Adsorption parameters for the surfactant inhibitor in 1.0 M HCl obtained from Langmuir adsorption isotherm at 30°C.

Temp., K	Adsorption isotherm	K mol ⁻¹ _{ads}	Slop	ΔG ^o _{ads} , kJ mol ⁻¹	R ²
303	Langmuir	40.26	1.20	-19.43	0.997

Therefore, ΔG^o_{ads} can be calculated according to equation (12). The degrees of surface coverage (θ) were evaluated from weight loss measurements using Eq. 2 and are given in Table 7. The regression coefficient R² = 0.999 suggests a good relation between C_{inh}/ θ and C_{inh}. The values of ΔG^o_{ads} recorded in Table 3.5. are negative, suggesting the spontaneity of the adsorption process and also show a strong interaction of the inhibitor molecule onto the C-steel surface. Generally values of ΔG^o_{ads} around of -20 kJ mol⁻¹ or lower are consistent with the electrostatic interaction between the charged molecules and the charged metal surface (physisorption), while those more negative than -40 kJ mol⁻¹ involve charge sharing or transfer from the inhibitor molecules to the metal surface to form a coordinate type of bond (chemisorption) [40, 41]. The calculated values of ΔG^o_{ads} for the investigated Gemini surfactant is - 19.4 kJ mol⁻¹ according to the reaction temperature. It suggests a physical adsorption might be occur [42].

Kinetic parameters:

The effect of temperature (30° - 50° C) on the performance of the surfactant inhibitor at different concentration of (25-150 ppm) for C- steel in 1.0 M HCl was studied using weight – loss measurements. Plot of log log k (corrosion rate) against 1/T (absolute temperature) for carbon steel in 1.0 M HCl and in the presence of various doses, Fig.8 gave a straight lines. The value of the slopes obtained at different temperatures permit the calculation of Arrhenius- activation energy (Ea*). Kinetic parameters for corrosion of C- steel were calculated from Arrhenius - type plot.

$$K = A \exp (-Ea^*/RT) \dots\dots\dots (12)$$

and transition state-type equation:

$$K = RT//N h \exp (\Delta S^*/RT) \exp (\Delta H^*/RT) \dots\dots (13)$$

The relation between log k/ T vs. 1/T gives straight line, and from its slop, ΔH* can be calculated and from its intercept ΔS* can be also computed

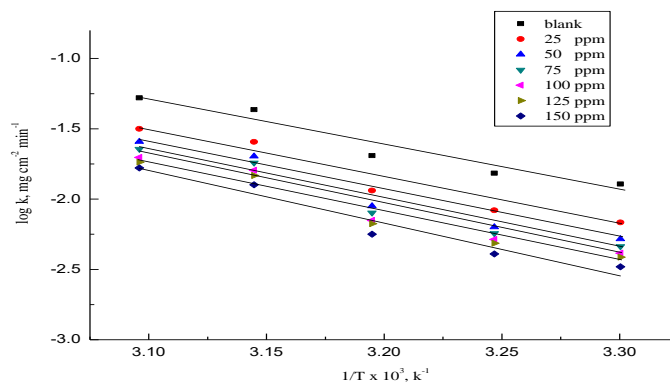


Fig. 8: Arrhenius plots (log k vs. 1/T) curves for C- steel dissolution in 1.0 M HCl in absence and presence of different concentrations of the surfactant molecule.

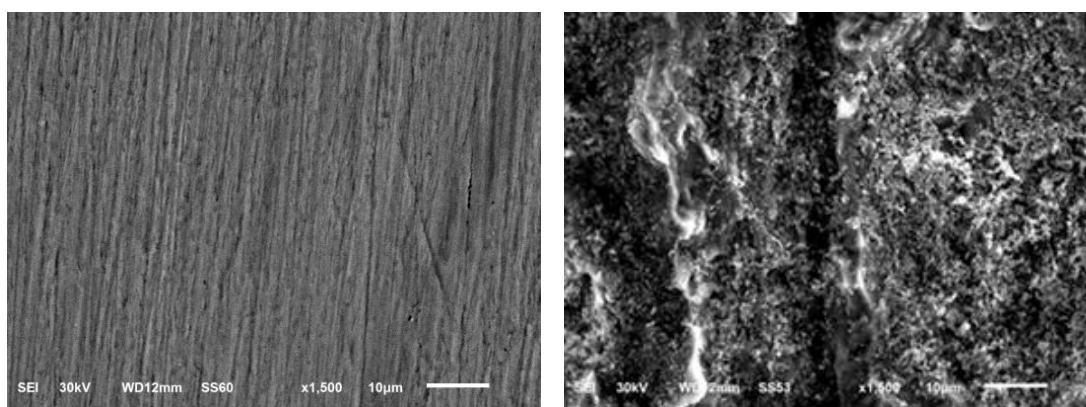
Table 3.6 showed the values of the apparent activation energy E_a^* , enthalpies ΔH^* and entropies ΔS^* for C- steel in 1.0 M HCl solution. The presence of the investigated surfactant increase the activation energies of C- steel reaction indicating strong adsorption of the surfactant molecules on the metal surface and the presence of these additives induces energy barrier for corrosion reaction and this barrier increase with the additives concentrations.

Table 8: Kinetic parameters for the dissolution of C- steel in absence and presence of different concentration of inhibitors in 1.0 M HCl.

Inhibitor	Conc., ppm	Activation parameters		
		E_a^* kJ/mol	ΔH^* kJ/mol	ΔS^* kJ/mol
Free acid (1.0 M HCl)	0.0	-62.72	-60.12	-83.94
Gemini surfactant inhibitor	25	-67.95	-65.35	-71.96
	50	-70.61	-68.02	-65.54
	75	-70.57	-67.97	-66.58
	100	-69.29	-66.68	-71.70
	125	-68.53	-65.93	-74.69
	150	-70.97	-68.37	-68.15

Surface examination using SEM–EDX techniques:

Scanning Electron Microscopy (SEM) studies:



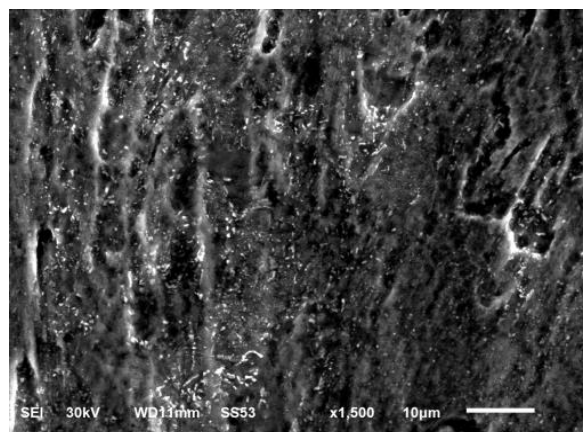
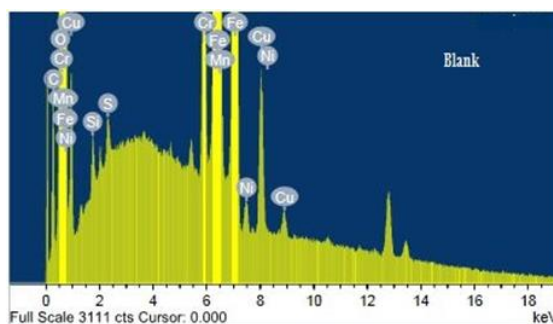
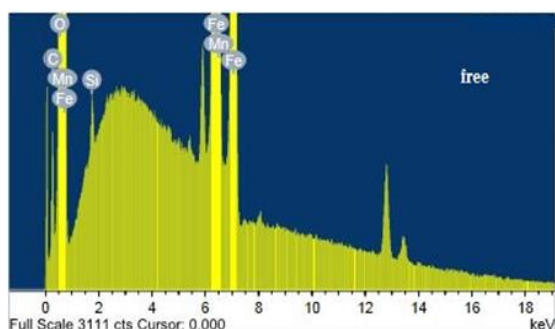


Fig. 9: SEM micrographs for carbon steel in absence and presence of 150 ppm for the surfactant inhibitor. (A) Free specimen, (B) blank (C-steel in 1.0 M HCl) and (C) in the presence of 150 ppm.

Fig.9 represents the micrograph obtained for C-steel samples in absence and presence of 150 ppm of the inhibitors after 150 minutes immersion. The resulting SEM reveal that the surface was strongly damaged in absence of the inhibitor, but in the presence of the optimum concentration of the Gemini surfactant molecules inhibitor there is much less damage of the surface. It is clear that, the specimen surface is smoother. We noted the formation of a film which is distributed in a random way on the whole surface of C-steel surface. This may be interpreted as due to the adsorption of the inhibitor on the C-steel surface incorporating into the passive film in order to block the active sites present on C-steel surface. Also it can be attributed to the involvement of inhibitor molecules in the interaction with the reaction sites of C-steel surface, resulting in a decrease in the contact between C-steel and the aggressive medium and sequentially exhibited excellent inhibition effect [43, 44].

Energy Dispersion analysis of X-Ray (EDX):

The EDX spectra were used to determine the elements present on the surface of C-steel and after 3 days of exposure in the uninhibited and inhibited 1.0 M HCl. Fig. 3.11. Shows the EDX analysis of C-steel only without the acid and inhibitor treatment The EDX analysis indicates that only Fe and oxygen were detected, which shows that the passive film contained only Fe₂O₃. Fig.10. Portrays the EDX analysis of C-steel in 1.0 M HCl only and in the presence of 150 ppm of the inhibitor. The spectra show additional lines, demonstrating the existence of C (owing to the carbon atoms present in inhibitor compound). These data show that the carbon and oxygen atoms covered the specimen surface. This layer is entirely owing to the inhibitor, because the carbon and oxygen signals are absent on the specimen surface exposed to uninhibited HCl. It is seen that, in addition to Mn, C and O were present in the spectra. A comparable elemental distribution is shown in Table 9



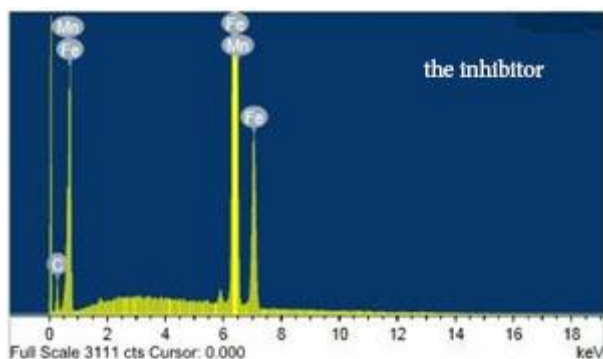


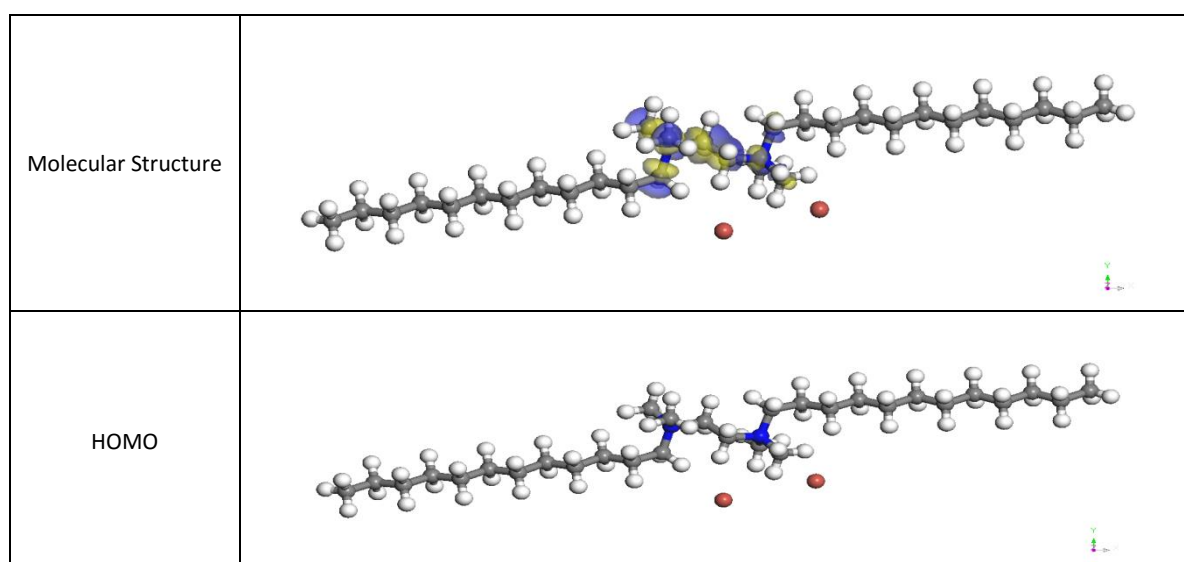
Fig. 10: EDX analysis on carbon steel in the presence and absence of the inhibitor compound for 3 days immersion.

Table 9: Surface chemical composition (wt %) of C-steel after 3 days of immersion in 1.0 M HCl without and with the optimum concentration of the studies inhibitor

Mass %	Fe	Mn	C	O	Si
Pure	86.97	0.64	6.03	6.06	0.30
Blank	77.56	1.77	8.95	8.58	0.30
Inhibitor	83.6	0.75	15.65	0.0	0.0

Quantum chemical parameters of investigated inhibitors compounds:

The E_{HOMO} indicates the ability of molecules to donate electrons to an appropriated acceptor with empty molecular orbital but E_{LUMO} indicates its ability to accept electrons. The lower the value of E_{LUMO} , the more ability of the molecule is to accept electrons [45]. While, the higher is the value of E_{HOMO} , of the inhibitor, the ease of its offering electrons to the unoccupied d-orbital of metal surface and the greater is its inhibition efficiency. Table (10) shows the quantum chemical calculation obtained by VAMP method. It is shown that a high energy E_{HOMO} is assigned for the inhibitor. The HOMO-LUMO energy gap, ΔE approach, which is an important stability index, is applied to develop theoretical models for explaining the structure and conformation barriers in many molecular systems. The smaller is the value of ΔE , the more is the probable inhibition efficiency that the compound had [46]. The dipole moment μ , the higher in the value of μ , which is in good agreement with the experimental data



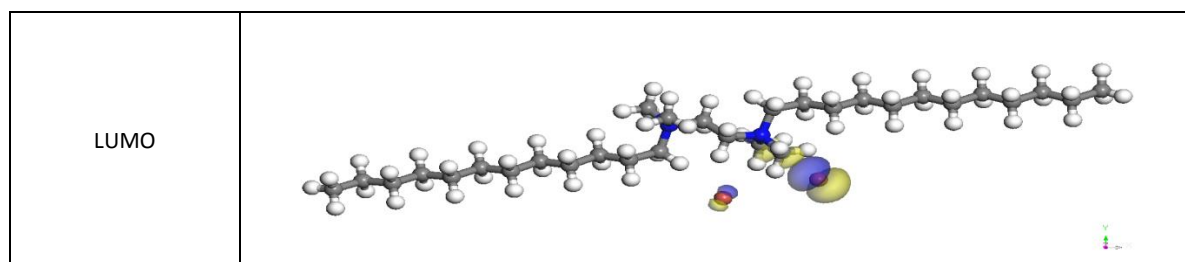


Fig. 10: The frontier molecular orbital density distribution for Gemini surfactant (HOMO and LUMO).

Table10: Quantum chemical properties calculated for the selected cationic Gemini surfactant.

Property	$E_{\text{HOMO}}(\text{eV})$	$E_{\text{LUMO}}(\text{eV})$	ΔE	η (eV)	σ (eV ⁻¹)	-Pi (eV)	χ (eV)	μ (Debye)
inhibitor	-10.586	-0.513	10.073	5.037	0.199	-5.55	5.929	38.548

Mechanism of corrosion inhibition:

The good inhibitive action of the tested cationic Gemini surfactant can be related to the fact that, quaternary ammonium salts have been used extensively as inhibitors against the corrosion of iron and steel, and this kind of organic molecules can be adsorbed on the metal surface because it can form a bond between the polar head groups of the inhibitor and the metal surface thereby, reducing the corrosion attack on the metal surface [47]. The inhibition efficiency data and Fig. 11. Show that the adsorption behavior of Gemini surfactant is more complicated than that of traditional surfactant because of the Gemini surfactant molecule consists of two hydrophilic groups and two hydrophobic groups that result in a complicated adsorption of this kind of surfactants onto the metal surfaces as previously published [48]. Three different modes of adsorption available to Gemini surfactant are shown in Fig. 11.

1- At low concentration, adsorption will take place by an electrostatic interaction between the two ammonium groups (N^+) and cathodic sites on the metallic surface (Fig. 11a).

2- On further increasing of inhibitor concentration, the inter hydrophobic chain interactions will become stronger, which may lead to desorption of one of the two hydrophilic ionic groups of the Gemini surfactant from the metal surface (Fig. 11 b) [49].

3- Both modes of adsorption (1) and (2) can co-exist, (Fig. 11 c). But in fact, the third mode should be more reasonable because of the interaction between molecules of Gemini surfactant, which explains the increase in the inhibition efficiency accompanied with increasing the concentration of the tested surfactant

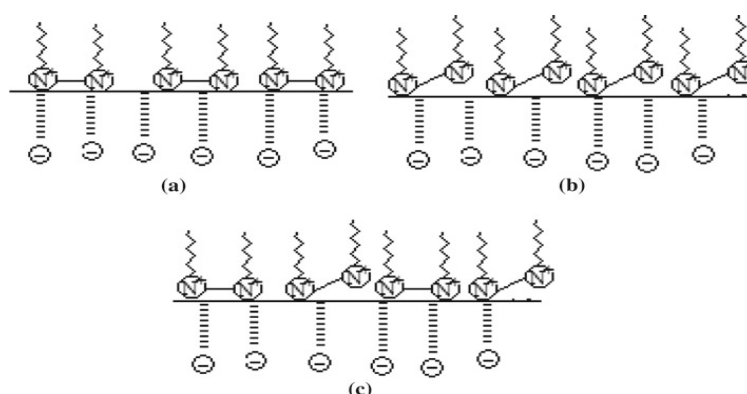


Fig. 11: Skeletal representation of the mode of adsorption of Gemini surfactant on carbon steel surface

CONCLUSIONS

- The investigated Gemini surfactant inhibits the corrosion rate of C-steel in 1.0 M HCl.

- The inhibition mechanism is attributed to the strong adsorption ability of the investigated surfactant on C-steel, forming a good protective layer, which isolated the surface from the aggressive environment and blocking its active sites.
- Adsorption of the investigated surfactants fits a Langmuir isotherm model.
- Results obtained from weightloss, dc polarization, ac impedance and EFM techniques are in reasonably good agreement and show increase inhibition efficiency with increasing inhibitor concentration.
- Polarization data shows that the investigated surfactants act as mixed-type inhibitor in 1.0M HCl

REFERENCES

- [1] S. Ghareba, and S. Omanovic, *Electrochimica.*, 2011;15:3890-3898.
- [2] D. Shuka, and V. K. Tyagi, *Cationic Gemini surfactants: A Review. J OleoSci.*, 2006;55: 381-390.
- [3] T. Alejo, M. D. Merchan and M. M. Velazquez, *Thin Solid Films*, 2011; 519:5689-5695.
- [4] L. G. Qiu, A. J. Xie, Y. H. Shen, *Appl. Surf. Sci.*, 2005; 246:1-5.
- [5] L. G. Qiu, Y. M. Wang and X. Jiang, *Corr. Sci.*, 2008;50:576-582.
- [6] L. G. Qiu, A. J. Xie, Y. H. Shen, *Mater. Chem. Phys.*, 2008;87:237-240.
- [7] Q. Chen, D. Zhang, R. Li, H. Liu and Y. Hu, *Thin Solid Films*, 2008;516:8782-8787.
- [8] W. Huang and J. Zhao, *J. Coll. Surf. A*, 2006;278:246-251.
- [9] M. A. Migahed, M. M. Attya, S. M. Rashwan, M.M. kamel and A. M. AlSabagh “, *Res. J. of Pharm. Biolog. and Chem. Sci.* 6 (2015) 1337 – 135.
- [10]
- [11] A. R. Tehrani Bagha, H. Bahrami, B. Movassagh, M. Arami, S. H. Arirshahi and F. M. Menger, *Coll. Surf. A*. 2007; 307:121-127.
- [12] M. A. Hegazy, M. Abdallah, H. Ahmed, *Corrosion Science* 2010;52:2897-2904.
- [13] L. B. Tang, G. N. Mu and G. H. Liu, *Corros. Sci.*, 2003;45:2251.
- [14] L. M. Vracarand, M. Drazic, *Corros. Sci.*, 2002; 44:1669-1680.
- [15] F. Bentiss, M. Lagrenée, M. Traisnel and J. C. Hornez, *Corros. Sci.*, 1999; 41: 789-803.
- [16] C. H. Hsu, F. Mansfeld, *Corrosion*, 2001;57 : 747-749.
- [17] R. Java her dashti, *How corrosion affects industry and life Anti-Corros, Meth. Mater*, 2000 ;47: 30-34.
- [18] K. S. Jacob and G. Parameswaran, *Corros. Sci.*, 2010;52:224-228.
- [19] M. A. Quraishi, D. Jamal, and M. Luqman, *Indian J. Chem. Technol.*, 2002;9:479-483.
- [20] H. A. Sorkhabi., B. Shaabani, and D. Seifzadeh, *Appl. Surf. Sci.*, 2005;239:154-164.
- [21] H. Ma, S. Chem, B. Yin, S. Zhao, X. Liu, *Corros. Sci.*, 2003; 45:867-882.
- [22] C. N. Cao, *Corrosion Electrochemistry Mechanism*, Chemical Industrial Engineering Press, Beijing, (in Chinese), 2004, 325.
- [23] M. El Achouri, S. Kertit, H.M. Gouttaya, B. Nciri, Y. Bensouda, L. Perez and, M. R. Infante, K. Elkacemi, *Prog. Org. Coat.*, 2001; 43 :267.
- [24] K. F. Khaled, *Electrochimica. Acta*, 2003; 48:2493.
- [25] A. Popova, E. Sokolova, S. Raicheva and M. Christov, *Corros. Sci.* 2003;45 : 33.
- [26] F. B. Growcock, J. H. Jasinski, *J. Electrochem. Soc.*, 198;136:2310.
- [27] U. Rammet and G. Reinhart, *Corros. Sci.*, 1987;27:373.
- [28] A. H. Mehaute and G. Grepy, *Solid State Ionics* 1983;17:9-10.
- [29] E. Machnikova, M. Pazderova, M. Bazzaoui and N. Hackerman, *Surf. Coat. Technol.*, 2008; 202:1543.
- [30] C. H. Hsu and F. Mansfeld, *Corrosion*, 2001;57:747.
- [31] M. Lebrini, M. Lagrenée, M. Traisnel, L. Gengembre, H. Vezin and F. Bentiss, *Appl. Surf. Sci.*, 2007:253:9267.
- [32] H. Duan, K. Du, C. Yan, F. Wang, *Electrochim. Acta*, 2006; 51 : 2898.
- [33] M. Mahdavian, S. Ashhari, *Electrochim. Acta*, 2010;55 : 1720
- [33] M. A. Migahed, E. G. Zaki, M. M. Shaban, *RSC advances*, 6 (2016) 71384 -71396
- [34] M. Goulart , A. E. Souza, C. A. M. Huitle, C. J. F. Rodrigues, M. A. M. Maciel, A. Echevarria , *Corros. Sci.*, 2013;67 : 281.
- [35] R. G. Kelly, J. R. Scully, D. W. Shoesmith, R. G. Buchheit, *Electrochemical Techniques in Corrosion Science and Engineering*, Marcel Dekker, Inc., New York, 2002 ,148.
- [36] Gamry Echem Analyst Manual, 2003.

- [37] R.W. Bosch, J. Hubrecht, W.F. Bogaerts, B.C. Syrett, *Corrosion*, 2001;57 :60.
- [38] P. Somasundaran, R. B. Grieves, *Advances in interfacial phenomena* of Marcel Dekker, 1988.
- [39] D. T. Wasan, M. Ginn and D.O.Shah, *Surfactants in process engineering*, NewYork, particulate/solution/gas systems. *AIChESymposium Series*, AIChESymp. Ser.1975 ,124.
- [40] O. C. Peter, Z. Yugui, *Corros. Sci.*, 2009; 51:850-859.
- [41] M. Behpour, S. M. Ghorei Shi, N. Soltani, M. Salavati, M. Niasari, Hamadani, A. Ghandomi, *Corros. Sci.*, 2008; 50 :2172.
- [42] E. Khamis, F. Belluci, R. M. Latanision, E.S.H. El-Ashry, *Corrosion*, 1991; 47 : 677.
- [43] R. A. Prabhu, T.V., Venkatesha, A.V., Shanbhag, G.M., Kulkarni, R. G. Kalkhambkar, *Corros.Sci.*, 2008;50 :3356-3362.
- [44] G. Moretti, G. Quartanone, A., Tassan, A., Zingales, *Wkst. Korros.*, 1994; 45:641-647.
- [45] C. Lee, W. Yang and R. G. Parr., *Phys. Rev. B*, 1988;37:785-789.
- [46] R. M. Issa, M. K. Awad and F. M. Atlam, *Appl. Surf. Sci.*, 2008;255:2433-2441.
- [47] N. A. Negm, A. M. Al Sabagh, M. A. Migahed, A. M. Abdel Bary, and H. M. El Din, *Corros. Sci.*, 2010;52:2122-2132.
- [48] L. G. Qiu, A. J. Xie, Y. H. Shen, Y.H., *Chem. Phys.*, 2005;91:269-273.
- [49] L. G. Qiu, A. J. Xie, Y. H. Shen, *Mater Chem. Phys.*, 2005;91:269.